Atmos. Chem. Phys. Discuss., https://doi.org/10.5194/acp-2019-7
Manuscript under review for journal Atmos. Chem. Phys.
Discussion started: 25 January 2019

Atmospheric Chemistry and Physics Discussions

Enhanced ice nucleation activity of coal fly ash aerosol particles initiated by ice-filled pores

Nsikanabasi Silas Umo[1], Robert Wagner[1], Romy Ullrich[1], Alexei Kiselev[1], Harald Saathoff[1], Peter G. Weidler[2], Daniel J. Cziczo[3,4], Thomas Leisner[1], and Ottmar Möhler[1]

[1]Institute of Meteorology and Climate Research - Atmospheric Aerosol Research, Karlsruhe Institute of Technology, Hermann-von-Helmholtz Platz 1, 76344 Eggenstein-Leopoldshafen, Germany
[2]Institute of Functional Interfaces, Karlsruhe Institute of Technology, Hermann-von-Helmholtz Platz 1, 76344 Eggenstein-Leopoldshafen, Germany
[3]Earth, Atmospheric and Planetary Sciences, Civil and Environmental Engineering, Massachusetts Institute of Technology, 77 Massachusetts Avenue 54-1324, Cambridge, MA 02139-4307, USA
[4]Now at: Purdue University, Department of Earth, Atmospheric and Planetary Sciences, 550 Lafayette St., West Lafayette, IN 47907, USA

Correspondence to: Nsikanabasi Silas Umo (nsikanabasi.umo@partner.kit.edu)

Abstract. Ice-nucleating particles (INPs), which are precursors for ice formation in clouds, can alter the microphysical and optical properties of clouds, hence, impacting the cloud lifetimes and hydrological cycles. However, the mechanisms with which these INPs nucleate ice when exposed to different atmospheric conditions are still unclear for some particles. Recently, some INPs with pores or permanent surface defects of regular or irregular geometries have been reported to initiate ice formation at cirrus temperatures via the liquid phase in a two-step process, involving the condensation and freezing of supercooled water inside these pores. This mechanism has therefore been labelled as pore condensation and freezing (PCF). The PCF mechanism allows formation and stabilization of ice germs in the particle without the formation of macroscopic ice. Coal fly ash (CFA) aerosol particles are known to nucleate ice in the immersion freezing mode and may play a significant role in cloud formation. In our current ice nucleation experiments with CFA particles, which we conducted in the Aerosol Interaction and Dynamics in the Atmosphere (AIDA) aerosol and cloud simulation chamber at the Karlsruhe Institute of Technology, Germany, we partly observed a strong increase in the ice-active fraction for experiments performed at temperatures just below the homogeneous freezing of pure water, which could be related to the PCF mechanism. To further investigate the potential of CFA particles undergoing PCF mechanism, we performed a series of temperature-cycling experiments in AIDA. The temperature-cycling experiments involve exposing CFA particles to lower temperatures (down to ~ 228 K), then warming them up to higher temperatures (238 K – 273 K) before investigating their ice nucleation properties. For the first time, we report the enhancement of the ice nucleation activity of the CFA particles for temperatures up to 263 K, from which we conclude that it is most likely due to the PCF mechanism. This indicates that ice germs formed in the CFA particles' pores during cooling remains in the pores during the warming and induces ice crystallization as soon as the pre-activated particles experience ice-supersaturated conditions at warmer temperatures; hence, showing an enhancement in their ice-nucleating ability compared to the scenario where the CFA particles are directly probed at warmer temperatures without temporary cooling. The enhancement in the ice nucleation ability showed a positive correlation with the specific surface area and porosity of the particles. On the one hand, the PCF mechanism could be the prevalent nucleation mode for intrinsic ice formation at cirrus temperatures rather than the previously acclaimed deposition mode. On the other, the PCF mechanism can also play a significant role in mixed-phase cloud formation in a case where the CFA particles are injected from higher altitudes and then transported to lower altitudes after being exposed to lower temperatures.

1. Introduction

Understanding the ice nucleation processes remains highly relevant to cloud formation and other applications in cryopreservation, geoengineering, bioengineering, material modifications, aviation, and in agriculture (John Morris and

Atmos. Chem. Phys. Discuss., https://doi.org/10.5194/acp-2019-7
Manuscript under review for journal Atmos. Chem. Phys.
Discussion started: 25 January 2019

Atmospheric Chemistry and Physics Discussions

Acton, 2013; Kiani and Sun, 2011; Murray, 2017). Ice nucleation by aerosol particles is known to modify cloud properties, hence, playing an important role in modulating the hydrological cycle and climate (Boucher et al., 2013; Seinfeld and Pandis, 2006). There are four mechanisms identified for primary heterogeneous ice nucleation in the atmosphere, which are the immersion, condensation, deposition, and contact modes (Pruppacher and Klett, 2010; Young, 1993). Immersion freezing occurs when an ice-nucleating particle (INP) initiates ice formation when completely immersed in a cloud droplet. Condensation freezing happens when ice nucleates as water is condensed on the INP whereas deposition nucleation occurs when water vapour directly forms the ice phase on a particle. Contact freezing is triggered when an INP comes in contact with a supercooled water droplet (from inside or outside) to initiate nucleation and subsequent freezing (Pruppacher and Klett, 2010; Vali et al., 2015). While immersion freezing is relevant in mixed-phase clouds (Murray et al., 2012), the deposition mode mechanism and homogeneous ice nucleation dominate cirrus cloud formation (Hoose and Möhler, 2012).

However, there is an ongoing debate on whether the direct deposition of water vapour on the surface of an INP is the real process behind ice formation, or whether it is rather the freezing of supercooled liquid water in the pores or crevices of such particle that later grows to form a macroscopic ice crystal (Marcolli, 2014 and the references therein). The mechanism is termed as the pore condensation and freezing (PCF) process. This phenomenon had been proposed in the past (e.g. Fukuta, 1966), but recently, there has been renewed interest in understanding this mechanism with more sophisticated experiments (Marcolli, 2017 and references therein). Generally, more recent studies have suggested that surface defects and pore properties are crucial factors in determining the ice nucleation mechanism of aerosol particles (Campbell et al., 2017; He et al., 2018; Kiselev et al., 2017; Li et al., 2018). For INPs with surface defects and pores to pre-activate in the atmosphere, the INPs need to undergo some level of processing at different atmospheric conditions before ice nucleation events. Here, we defined pre-activation as the process whereby ice germs are formed in the particle pores when such particles are temporarily exposed to a lower temperature (Wagner et al., 2016a). In addition, the recycling of aerosol particles through regions of varying relative humidity in the atmosphere could also influence their ice nucleation mechanisms (Heymsfield et al., 2005; Knopf and Koop, 2006). Some laboratory experiments have been carefully performed to investigate the pre-activation processes to gain a better understanding of the possible scenarios when the PCF mechanism can contribute to pre-activation. In such experiments, pre-activated pores in the particles have been observed to enhance the particles' ice-nucleating properties (Marcolli, 2017; Wagner et al., 2016b). For example, Wagner et al. (2016) reported pre-activation of various particles such as Zeolite, Illite, desert dust from Israel and Arizona, soot, and Icelandic volcanic ash by the PCF mechanism. These particles all showed varying degree of improvement in their inherent ice nucleation abilities via the PCF mechanism. The ice formation via this mechanism is restricted to a certain pore size range (5 – 8 nm) (Wagner et al., 2016a). Aside from pre-existing porous materials, organic-related aerosol particles such as ultra-viscous or glassy aerosols have shown a considerable augmentation in their ice nucleation activities when pre-processed in clouds (Wagner et al., 2012). This is attributed to the formation of porous particles during the ice-cloud processing. These studies established that in clouds, ice can easily form on pre-activated particles by depositional growth at $RH_{ice} > 100$ % without any specific activation threshold, whereas definite ice active sites are required for a classical deposition nucleation process to occur. Aside from pores on INPs, the extent of surface defects or topography of the particles may also influence their ice formation potential (Campbell et al., 2017; Campbell and Christenson, 2018; Kiselev et al., 2017; Li et al., 2018; Whale et al., 2017). However, it is not very clear how this mechanism takes place.

A better understanding of the PCF mechanism by different INPs can provide better insights into the potential contributions of these INPs to the global ice budget. Coal fly ash (CFA) is one group of aerosol particles that are constantly emitted into the atmosphere from the energy production by coal burning (Manz, 1999). About 500 - 800 million tonnes of CFA aerosol particles are produced annually (Adams, 2018; Heidrich et al., 2013; Joshi and Lohita, 1997) and a significant amount of this

Atmos. Chem. Phys. Discuss., https://doi.org/10.5194/acp-2019-7
Manuscript under review for journal Atmos. Chem. Phys.
Discussion started: 25 January 2019

proportion is injected into the atmosphere – hence, they could contribute to heterogeneous ice formation in clouds. Previously, CFA particles have been shown to nucleate ice in the immersion mode (Grawe et al., 2016, 2018; Umo et al., 2015). However, there are variabilities in the ice nucleation activities of the different CFA samples reported, which could be due to the difference in mineralogical compositions; as well as variabilities in the actual freezing mechanisms, which could be influenced by surface defects or porosity of the particles. The ice-nucleating behaviour of CFA particles, when exposed to various atmospheric conditions, is still unclear and requires further investigations.

In this study, we investigated the ice nucleation behaviour of different CFA particles at temperatures greater than 238 K. When we tested the ice nucleation ability of these particles at temperature just below the homogeneous freezing of pure water, one of the CFA samples showed a high fraction of ice-active particles at a low relative humidity (S_{ice} = 1.02) in apparent contrast to intrinsic ice-nucleating abilities of CFA. This result was indicative of a PCF mechanism as put forward by Marcolli (2014) that a variety of aerosol particle types showed a sudden increase in their IN ability just below the homogeneous freezing temperature. Following our preliminary observations, we decided to prove whether the CFA particles are also prone to the PCF mechanism by adopting a temperature-cycling protocol which is described in full in section 2.6. Here, we report the ice nucleation behaviour of different CFA aerosol particles when temporarily exposed to lower temperatures at ice-subsaturated conditions and then probed at warmer temperatures. The results were then compared to their intrinsic ice-nucleating abilities at similar temperatures to understand the potential freezing mechanism by CFA in such conditions. The results from these new laboratory measurements are presented in this report. It is organized in the following sections: the experimental procedure adopted for this study, the description of the results, and the potential atmospheric implications of the new results to ice formation in mixed-phase clouds as well as possible pathways in cirrus clouds. The article concludes by pointing out some future perspectives for research on this subject.

2. Materials and Experimental Methods

2.1 Samples

In this study, we used five coal fly ash (CFA) samples that were collected from electrostatic precipitators (EPs) of five different power plants - four in the United States of America and one in the United Kingdom. The four CFA samples from the USA were supplied by the Fly Ash Direct Ltd©, USA. However, the CFA samples were sourced from the following power plants: Clifty Creek Power Plant in Madison, Indiana (hereafter labelled as, CFA_Cy), Miami Fort Generating Station in Miami Township, Ohio (hereafter labelled as, CFA_Mi), Joppa Generating Station in Joppa, Illinois (hereafter labelled as, CFA_Ja), and J. Robert Welsh Power Plant in Titus County, Texas (hereafter labelled as, CFA_Wh). These are the same set of samples also studied and reported in Garimella (2016). The UK coal fly ash sample was obtained from one of the major power plants in the UK and is referred to as CFA_UK throughout this report. The name of the UK power plant prefers anonymity; hence, no specific name is mentioned here. First, the raw CFA_UK sample was sieved with a Fritsch Sieve set-up (Analysette 3, 03.7020/06209, Germany) to obtain a 0 – 20 µm diameter size fraction, which was later used for the experiments.

2.2 AIDA chamber

All investigations were carried out in the Aerosol Interactions and Dynamics in the Atmosphere (AIDA) aerosol and cloud simulation chamber. This is an 84 m^3 sized aluminium vessel sitting in a temperature-controlled housing, where the pressure, temperature, and the relative humidity are well-controlled depending on the experimental requirements. In addition, a suite of instruments is connected to the chamber for direct in situ measurements or extractive measurements after sampling air from the chamber. A detailed description of the AIDA chamber and its instrumentation has been previously reported in

Atmos. Chem. Phys. Discuss., https://doi.org/10.5194/acp-2019-7
Manuscript under review for journal Atmos. Chem. Phys.
Discussion started: 25 January 2019

Atmospheric Chemistry and Physics Discussions

various works (including but not limited to Möhler et al., 2003; Steinke et al., 2011; Wagner et al., 2009). Here, a brief overview of the devices which were employed in our study is highlighted.

A combination of an aerodynamic particle sizer (APS) (TSI GmbH, USA), and a scanning mobility particle sizer (SMPS) (TSI GmbH, USA) was used to measure the size distribution of the CFA aerosol particles in the AIDA chamber. The SMPS instrument measures in the size range of (13.3 – 835.4 nm), while the APS has a larger detection size range (0.5 – 20 µm). Both instruments were operated at the same time to obtain the full-size distribution spectrum of the particles. A condensation particle counter (CPC3010, TSI, USA) was used to measure the number of aerosol particles in the chamber per volume. We also deployed two optical particle counters (OPCs) (WELAS 2000, PALAS GmbH, Germany), which were connected to the base of the chamber to sample aerosol particles, cloud droplets, and ice crystals and measure their respective optical sizes. Each of the OPCs had a different detection limit (0.7 – 46 µm and 5 – 240 µm). The data obtained from the WELAS systems was later used to calculate the ice particle number concentration in the chamber during expansion cooling experiments with an uncertainty of ± 20 %. The water vapour concentration in AIDA at every stage of the experiment was measured with tunable diode laser (TDL) spectrometers, from which the relative humidities with respect to water (RH_w) and ice (RH_{ice}) were calculated with ± 5 % uncertainty (Fahey et al., 2014). The spatial and temporal homogeneity of the temperatures in the AIDA chamber is better than ± 0.3 K. In this report, the mean gas temperatures will be given throughout the manuscript.

2.3 Aerosol generation and injection into AIDA

CFA aerosol particles were injected into the AIDA chamber with a rotating brush generator (RBG, RBG1000, PALAS GmbH, Germany) connected to the chamber with cleaned Teflon and stainless-steel tubing. We coupled the RBG to two cyclones placed in series to eliminate particles larger than 3 µm in diameter). The aim was to obtain smaller sized particles (< ~ 2.5 µm), which are more atmospherically relevant, especially for long-range transportation in the atmosphere (Prospero, 1999).

2.4 Morphology of CFA – sampling and imaging

Samples of CFA particles were collected on a nuclepore filter (25 mm diameter, 0.02 µm pore size, Whatman®, USA) from the AIDA chamber. The sampling was carried out with a mass flow controller (MFC, Tylan®, UK) running at 2 L Min^{-1} for 30 mins. The loaded filters were sputter-coated with 1 nm platinum to improve the conductivity, and the images were taken with an environmental scanning electron microscopy (ESEM) (FEI Quanta 650 FEG). A different model of ESEM (ThermoFisher Scientific Quattro S) was used for the US CFA samples. With this new ESEM model, we were able to obtain images of the CFA particles under grazing viewing angles similar to 3-D images (see Fig. 1).

2.5 Surface area and pore size measurement

We adopted the Brunauer–Emmett–Teller (BET) method (Brunauer et al., 1938) to measure and analyse the specific surface areas (SSAs) of the 5 CFA samples. The CFA samples were degassed at ~ 368 K for 24 hours before measuring the molecular adsorption on the particles (a 5-point BET model was used). During the degassing process < 8.5 % mass loss was recorded for all the CFA samples. Specifically, we used Argon gas (87.3 K) as the adsorbent instead of the standard Nitrogen gas, hence, we tagged it BET_{Ar}. Argon gas provides better adsorption for the estimation of SSA because of its monatomicity and non-localization of the adsorbent during adsorption (Rouquerol et al., 2014; Thommes et al., 2015). This measurement was performed with an Autosorb 1-MP Instrument (Quantachrome, Germany). The pore size volumes were calculated with models based on DFT/Monte Carlo methods assuming a mixture of spherical and cylindrical pores on an oxygen-based substrate (Landers et al., 2013; Thommes et al., 2006). The SSA (m^2/g) from the BET_{Ar} measurements and the calculated

Atmos. Chem. Phys. Discuss., https://doi.org/10.5194/acp-2019-7
Manuscript under review for journal Atmos. Chem. Phys.
Discussion started: 25 January 2019

Atmospheric Chemistry and Physics Discussions

pore volumes for all the CFA samples are presented in Table 1.

2.6 Temperature-cycling and ice nucleation experiments in the AIDA chamber

CFA aerosol particles were first injected into the chamber filled with synthetic air set at a particular temperature - hereafter, referred to as start temperature (T_{start}) - and mixed with the aid of a big fan installed at the lower level of the chamber. After the injection of CFA particles into the AIDA chamber, the CFA particles were probed in two different ways. In the first type of experiments, the particles' intrinsic ice nucleation ability was tested at temperatures between 261 K and 228 K by means of an expansion cooling cycle. For this purpose, the pressure of the chamber was reduced with the aid of a vacuum pump (Möhler et al., 2005). Cooling and the concomitant increase of the relative humidity triggered the droplet activation of the particles, and a subset of the CFA particles nucleated ice via immersion freezing during continued pumping. Pumping was stopped when the minimum gas temperature was reached.

In the second type of experiments, a temperature-cycling and freezing (TCF) protocol was adopted. Previously, this method had been used for similar experiments with other aerosol types in the AIDA (Wagner et al., 2012, 2016a). In the TCF procedure, the CFA particles were injected into the AIDA chamber (~ 1300 - 1600 particles per cm^3) at ~ 253 K and cooled to ~ 228 K. During the cooling process, a rate of 5 K h^{-1} was achieved. The CFA aerosol particles were then warmed to 253 K (or the desired T_{start}) at 2.5 K h^{-1}, as described by Wagner et al. (2016). During the entire cooling and warming process (Fig. 2), the relative humidity prevalent in the AIDA chamber was slightly below ice saturation, as controlled by an ice layer on the inner chamber walls. After warming, the particles' ice nucleation ability was probed in an expansion cooling run as described above. Details of the various experiments that we conducted are shown in Table 2.

3. Results and Discussions

The freezing experiments data showing the inherent ice-nucleating ability of the CFA particles are shown in Fig. 3 (CFA_UK), in the first column (A) of Fig. 5 (CFA_Cy), as well as summaries for CFA_UK (Fig. 6) and CFA_Mi, CFA_Ja, and CFA_Wh (Fig. 7). Each column of figures 3 and 5 has 3 panels. The top panel represents the pressure and the temperature profiles before, during, and shortly after the expansion. For each start temperature (T_{start}), the expansion started at ~ 1000 hPa down to where the maximum RH (see the middle panel) was obtained. The point, where the pressure starts rising, indicates when the freezing experiment was stopped. The middle panel shows the relative humidity data with respect to both water and ice denoted as RH_w and RH_{ice}, respectively. The bottom panel shows the optical diameters of the aerosol particles, cloud droplets, and ice crystals inferred from the OPCs. The CFA aerosol particles are shown by the dots at the beginning of the plot (α, see Fig. 3A), just before the pumping starts, mostly they are < ~ 10 µm. The particles activated into droplets are indicated by the denser cloud of data points with much bigger sizes, which shows that the CFA particles took up water, got immersed and increased in size (denoted by □, Fig. 3A). Finally, in the case where CFA particles had been activated into cloud droplets, the nucleated ice particles in the later course of the expansion run are indicated by the data points with sizes above the dense cloud of supercooled water droplets (see an illustration in Fig. 3C, denoted by □). In the cirrus regime or after temperature-cycling, the CFA particles can also directly form ice without going through the droplet activation phase (Fig. 3D). We used a size threshold, empirically set for each experiment, to separate the ice particles from both the CFA seed aerosol particles and the activated cloud droplets, similar to the approach reported in previous AIDA experiments (Steinke et al., 2016; Suski et al., 2018; Ullrich et al., 2017).

Here, we used the ice-active fractions to compare the data from the various experiments performed in this study. The fraction of ice frozen (i.e., the ice-activated fraction, f_{ice}) was calculated as the number of ice particles detected divided by the total

Atmos. Chem. Phys. Discuss., https://doi.org/10.5194/acp-2019-7
Manuscript under review for journal Atmos. Chem. Phys.
Discussion started: 25 January 2019

Atmospheric Chemistry and Physics Discussions

number of unfrozen aerosol particles or unfrozen droplets (Vali, 1971). The f_{ice} in each experiment is also plotted (Figs. 3 – 5).

The results from the ice nucleation experiments are presented as follows. We started with the inherent ice nucleation behaviour of the CFA samples (section 3.1); followed by the enhancement of their ice nucleation activities due to pre-activation by the PCF mechanism (section 3.2), and finally, we discussed potential implications of this mechanism for cloud formation by CFA INPs, especially those that have undergone similar temperature-cycling in the atmosphere (section 3.3).

3.1 Ice-nucleating activity of CFA particles

We start our discussion with the CFA_UK particles. When probed in an expansion cooling run at T_{start} = 261 K, the ice-active fraction is below the detection limit of 0.02 % (Fig. 3A). However, at T_{start} = 253 K, about 0.19 % of the particles nucleated ice in the immersion mode at the lowest temperature reached (245 K) (Fig. 6). The activated fraction (f_{ice}) at T_{start} = 245 K increased by a factor of 10 at the minimum temperature reached. At t = ~ 300 s, the homogeneous freezing mode kicked in (see the illustration in Fig. 3C). In our analyses, ice particles detected just before, during, and after such events were omitted from the ice particle counts. In summary, the CFA_UK particles were thus observed to be active in the immersion freezing mode at temperatures below 253 K down, however, the ice-activated fractions were rather low and exceeded 1% only at temperatures very close to the homogeneous freezing threshold. The homogeneous freezing threshold observed in our experiments agreed with previous reports (Benz et al., 2005; Schmitt, 2014). In contrast, for the experiment at T_{start} = 228 K (Fig. 3D), more than 70 % of the aerosol particles nucleated ice directly from the CFA_UK particles at very low supersaturation. This means that within a change of only 8 K in T_{start}, the ice-activated fraction increased by almost 2 orders of magnitude. A similar increase in the heterogeneous ice nucleation ability has been previously observed for zeolite and illite particles (Wagner et al., 2016a), and temperature-cycling experiment with these particles have substantiated that the PCF mechanism is the most likely explanation for the sudden increase of the particles' ice nucleation behaviour below the homogeneous freezing temperature of supercooled water. Following the experiment at T_{start} = 228 K, we hypothesized that PCF may also be the dominant nucleation pathway for the CFA particles. To verify this hypothesis, we adopted the TCF approach as discussed in section 3.2.

Other CFA samples studied here – CFA_Cy, CFA_Mi, CFA_Ja, and CFA_Wh were also tested for their intrinsic ice-nucleating properties in the immersion freezing at T_{start} = 251 K, 250 K, 251 K and 248 K, respectively (Figs. 5 and 7). The maximum ice-activated fraction ($f_{ice,\ max}$) for CFA_Cy at T_{start} = 251 K was ~ 1.7 % while CFA_Mi at T_{start} = 250 K reached 1.5 % f_{ice}. CFA_Ja showed ~ 16 % f_{ice} at T_{start} = 251 K while ~ 27 % f_{ice} at T_{start} = 248 K was observed for CFA_Wh. Due to the higher ice-activated fractions in the latter two experiments, the lifetime of the cloud droplets in the chamber was significantly reduced due to the Bergeron-Findeisen process. The droplet freezing in both samples (CFA_Ja and CFA_Wh) was relatively fast, which led to a rapid growth of the ice crystals formed; hence, the water content in the chamber was rapidly depleted (i.e. the ice took up water from the activated droplets to grow to larger sizes). Further analyses on the distribution of the ice nucleation active sites densities of these CFA particles is outside the scope of the current report and will be presented in a separate communication.

Coal fly ash particles from other sources have been reported to nucleate ice at much warmer temperatures. Previously studied CFA particles were suspended in deionized water before ice nucleation properties were investigated on cold stage set-ups. For example, a particular sample from one of the UK power plants was reported to nucleate ice in the immersion freezing mode already starting at 257 K (Umo et al., 2015). This sample also showed a steep curve in the f_{ice}, indicating the presence

Atmos. Chem. Phys. Discuss., https://doi.org/10.5194/acp-2019-7
Manuscript under review for journal Atmos. Chem. Phys.
Discussion started: 25 January 2019

of unique ice active sites which may be similar to what we observed in CFA_Ja and CFA_Wh. Grawe et al (2018) reported even higher freezing temperatures (from 265 K) for CFA particles obtained from a power plant in Germany. This again was attributed to the unique composition of CFA samples. Both studies can access warmer freezing temperatures for INPs than the dry generation method that our system is designed for. In another study, ice formation by particles in a plume from a coal-fired power plant had been detected from 263 K (Schnell et al., 1976). The particles in the plume were not well characterized, hence, it may have contained any other ambient aerosol particles.

Generally, for investigations in a freezing system that requires a dry generation method, much lower temperatures are reported as inherent ice-nucleating temperatures of CFA as INPs. A study of CFA samples from Germany in a laminar flow tube in Leipzig called Leipzig Aerosol Cloud Interaction Simulator (LACIS) showed ice nucleation from ~ 247 K - 236 K (Grawe et al., 2016, 2018). This study attributed the ice nucleation behaviour of the CFA particles to the Quartz composition of the CFA; however, it should be noted here that the particle sizing of the CFA samples used in their study is different from the size range used in our study. In this work, the average median particle diameter was 0.58 µm for our CFA samples theirs was size-selected to 0.3 µm. This can also impact on the behaviour of INPs (Welti et al., 2009). First, we should state here that these particles are from different sources, hence, they might have different mineral compositions as well as surface properties. Aerosol compositions and surface properties have been clearly established to influence the ice nucleation behaviour of INPs (Isono and Ikebe, 1960; Mason and Maybank, 1958). Second, the different measurement techniques applied in each study can also introduce some differences (Hiranuma et al., 2018). In comparison with other aerosol types, the ice nucleation activities of CFA particles in the immersion freezing mode are considerably higher than e.g. soot particles (Mahrt et al., 2018), but less active compared to some biological materials (Suski et al., 2018). Their ice-nucleating abilities are similar to the ice-nucleating potential of some mineral components of desert or agricultural soil dusts (Grawe et al., 2018; Umo et al., 2015).

3.2 Enhancement of the ice-nucleating properties of CFA particles by temperature-cycling

In the previous section, we reported only the inherent ice nucleation behaviour of CFA particles. Here, we show the results for CFA particles that were temporarily exposed to a lower temperature (228 K) before the expansion cooling experiments were conducted (Figs. 4 & 5). Freezing data after the temperature-cycling and freezing (TCF) procedure are presented in Fig. 4A - C and Fig. 5B.

After the TCF process, experiments were conducted with the processed CFA_UK particles following the schematic on Figure 2. Specifically, we conducted experiments in this order: T_{start} = 250 K → 254 K → 264 K as shown in Figure 4. At T_{start} = 250 K, we clearly observed an increase in the f_{ice} of the CFA_UK particles (up to 12 %) compared to the unprocessed CFA_UK particles that only showed f_{ice} of 1.6 % at T_{start} = 245 K, which was even at a lower start temperature. This occurred at a lower RH_{ice} = ~ 105 % than the experiment with unprocessed CFA_UK particles which RH_{ice} = ~ 130 % (corresponding to water saturation). This means that there was a change in the ice nucleation mode in comparison with the unprocessed CFA_UK particles in the same T_{start} range. For the processed CFA_UK particles, there was no droplet activation before the emergence of ice, i.e., ice formation cannot be ascribed to 'classical' immersion freezing (Fig. 3A - C). Rather, the ice particles observed were formed directly on the pre-activated CFA_UK particles. Following the history of these particles, we suggest that the ice particles may have been formed by the depositional growth on the ice germs formed in the pores of the particles during temperature-cycling.

After the first expansion at T_{start} = 250 K, we warmed the chamber to 254 K and performed another expansion cooling run.

Atmos. Chem. Phys. Discuss., https://doi.org/10.5194/acp-2019-7
Manuscript under review for journal Atmos. Chem. Phys.
Discussion started: 25 January 2019

Atmospheric Chemistry and Physics Discussions

We conducted two independent experiments for the processed CFA_UK particles at T_{start} = 254 K, only one is shown in Fig. 4B. The ice-activated fraction decreased by a factor of 2 compared to the run at T_{start} = 250 K (f_{ice} = ~ 3 – 5 %), but was still significantly higher than what was observed for the unprocessed CFA_UK particles at a similar temperature (f_{ice} = 0.23 % at T_{start} = 253 K). Ice formation by the processed CFA_UK particles again occurred by the depositional growth mode at low ice supersaturation (RH_{ice} = 107 %), whereas the much smaller ice nucleation mode of the unprocessed particles was due to immersion freezing at water-saturated conditions (corresponding to RH_{ice} = 124%) (Fig. 3).

Afterwards, the processed CFA_UK aerosol particles were warmed to T_{start} = 264 K for another expansion cooling run (Fig. 4C). At this temperature, the ice nucleation ability of the unprocessed CFA_UK particles was below our detection limit of 0.02 % for f_{ice}. For the processed CFA_UK particles, however, an ice-activated fraction of 1.2 % was observed. In contrast to the runs conducted at 250 K and 254 K, the ice cloud was not formed at low supersaturation values with respect to ice, but appeared just at the instant of droplet activation. Given the absence of any ice formation for the unprocessed particles, it is highly probable that the nucleation mode of the processed CFA_UK particles, although being similar to a classical immersion freezing mode, is in fact related to ice growth from an existing ice germ formed during temperature-cycling. Such ice formation modes have already been observed for other particle types in similar scenarios e.g. (Mahrt et al., 2018; Wagner et al., 2016b), and have been ascribed to the condensational growth of the ice germs formed in the pores or crevices of these particles. Figure 6 shows the summary of the ice nucleation enhancement of CFA_UK particles described above with their specific temperatures and the corresponding f_{ice}. For the unprocessed CFA particles, temperatures at the maximum f_{ice} were plotted. It is clear that for the processed CFA_UK particles, the f_{ice} values are significantly higher than the unprocessed particles at a similar T_{start}.

In contrast to the CFA_UK particles, the CFA particles from the USA power plants showed less modification of their ice nucleation ability after the temperature-cycling process. For none of these particle types, a distinct depositional ice growth mode as shown in Figs. 4A and B for the CFA_UK particles was observed. However, some particle types revealed an improved ice nucleation ability due to the condensational ice growth mode, as exemplified in Fig. 5 for the CFA_Cy particles. Whereas the ice-activated fraction of the unprocessed CFA_Cy particles remained below 0.5 % for temperatures above 244 K (Fig. 5A), the particles subjected to temperature-cycling showed ice formation with f_{ice} > 0.5 % already at 249 K (Fig. 5B). Similar to the experiment with CFA_UK at 264 K (Fig. 4C), this ice mode was instantaneously formed upon droplet activation, i.e., is most likely related to a condensational ice growth mode. CFA_Cy showed a tiny depositional growth mode indicated by a few ice particles detected before the droplet activation (Fig. 5B). To better illustrate the partly small differences in the ice nucleation ability of the CFA particles from the USA with and without temperature-cycling, we summarize in Fig. 7 the ice-activated fractions as a function of temperature for both the expansion cooling runs with processed and unprocessed particles. For the corresponding data of the CFA_Cy particles as discussed above, there is a clear shift of the ice nucleation spectrum towards warmer temperatures after temperature-cycling. For the other particle types, the difference is much less pronounced. At T_{start} = 253 K, the f_{ice} for CFA_Cy particles after the pre-activation process was ~ 0.86 % slightly lower than what was observed for the unprocessed CFA_Cy particles. However, the ice particles were detected at the instant that water saturation was reached (see the short-dashed blue line in Fig. 5B). Hence, condensational growth may be contributing to the ice formation although with less effect compared to the observations with processed CFA_UK particles. Further warming to T_{start} = 257 K, did not show any significant ice nucleation activity (~ 0.03 %). At this start temperature, the particles have lost their potential to retain their ice germs in their pores. Compared to the CFA_UK pre-activated particles that retained its ice nucleation ability even up to 264 K, and possibly at warmer temperatures, however, we did not explore this limiting threshold.

Atmos. Chem. Phys. Discuss., https://doi.org/10.5194/acp-2019-7
Manuscript under review for journal Atmos. Chem. Phys.
Discussion started: 25 January 2019

Atmospheric Chemistry and Physics Discussions

Enhancement of the ice nucleation behaviour of pre-activated CFA_Mi particles was not observed for experiments at start temperatures of 249 K and 255 K (Fig. 7). The $f_{ice,\ max}$ decreased from ~ 1.5 % at T_{start} = 250 K for unprocessed CFA_Mi particles to 0.4 % at T_{start} = 249 K after pre-activation, and even less ~ 0.1 % at T_{start} = 255 K (Fig. 7). This may be due to lack of sustainable ice germs in the pores or the crevices of these particles. Without the TCF procedure, ice nucleation was not observed at all at this higher temperature (255K) for CFA_Mi aerosol particles. Which suggests that the improved high-temperature ice nucleation ability might have been triggered by ice germs that were formed and preserved in the pores of the CFA_Mi INPs via the PCF mechanism when they were temporarily exposed to 228 K at ice-subsaturated conditions. This confirms that special pores are required for ice preservation.

For the CFA_Ja pre-activated particles, ice formation was observed at the instant of droplets activation, i.e. during the expansion process for experiments at 249 K and 256 K start temperatures (Fig. 7). Again, for the processed CFA_Ja particles, no appreciable enhancement of its ice formation abilities was observed as the f_{ice} at T_{start} = 249 K was 2 % at RH_{ice} = ~125 %. The sharp decrease in the RH is an indication of the fast growth of the formed ice particles, hence, depleting the water contents of the particles that were activated into droplets – a typical Wegener-Bergeron-Findeisen process (Storelvmo and Tan, 2015). After warming the processed CFA_Ja particles to T_{start} = 256 K, the amount of ice formed reduced by a factor of 6 (f_{ice} = ~ 0.9 %). We cannot completely rule out that the actual formation mechanism in both scenarios after the temperature-cycling is not via a condensational freezing pathway. One thing is extremely clear that the ice particles were detected as soon as water saturation was reached or at the instant of droplets activation. This was not seen for the unprocessed CFA_Ja particles; after reaching water saturation, there was a time lag before ice particles were detected.

A closer look at the pre-activated CFA_Wh particles showed an improved ice formation after the temperature-cycling experiment though not as significant as the processed CFA_UK sample. At T_{start} = 249 K after the pre-activation process, more ice particles were observed at the instant of the droplet activation and this totally suppressed droplet formation in the chamber. We suggest that there was strong competition between immersion ice formation and depositional growth in this case. At the RH_{max}, this was followed by a steep and narrow decrease in the RH. Again, we observed a few ice particles even before some few particles were activated into a cloud droplet. In short, ~ 4 % (RH_{ice} = 128 %) of the aerosol particles formed ice particles although at a fast rate, which rapidly grew and depleted the activated droplets in the chamber. When the system was warmed up to T_{start} = 256 K, the f_{ice} reached 3 % at a much lower RH_{ice} =120 %. Again, some ice particles were observed as the particles were activated into droplets. A plot of the ice-activated fraction for the unprocessed and the processed experiments with CFA_Wh particles does not show a higher fraction but clearly, ice formation occurred in a shorter temperature step for the processed CFA_Wh (Fig. 7). It could be that for an already ice-active CFA particles such as CFA_Wh, pre-activation by PCF may not be very important compared to other particles that are less ice-active.

The degree of ice nucleation enhancement by CFA particles differs from sample to sample. The enhancement capability of the CFA samples studied here are in this order: CFA_UK>>>> CFA_Cy>CFA_Wh>>CFA_Ja=CFA_Mi. The comparison is based on the start temperature, f_{ice}, and the relative humidity which summary is given in Figs. 6 & 7. Morphology, surface area, and pore volume are important parameters influencing the efficiency of the PCF mechanism. In the following, we discuss whether differences in these properties can account for the different behaviour of the CFA particles after temperature-cycling.

The morphology of the five samples is given in Fig. 1 for selected typical particles. The images showed that the CFA particles have some degree of roughness, coatings, layers, and mesh-like structures on their surface. Although the overall particle habit

is spherical, as many electron micrographs of CFA have shown (Blissett and Rowson, 2012; Fisher et al., 1978), they have no smooth surface. Of the 5 CFA samples, CFA_UK had the highest degree of deformity on the surface as indicated in Fig. 1a - f. We attempted to focus into the surface (up to ~ 50 - 100 nm resolution) to identify the potential pores and crevices but it was difficult to have a clear view of the pores (Fig. 1c & f). Classical nucleation theory and empirical calculations have shown that pore diameters of about 5 – 8 nm (mesopores) contribute to a particle's pre-activation ability at ice sub-saturated conditions (Marcolli, 2014; Wagner et al., 2016a). To better understand the nature of the CFA surfaces, we measured the specific surface area (SSA) of the sieved bulk samples (0 – 20 µm) using the BET method but with Argon gas rather than Nitrogen (Gregg et al., 1967; Thommes et al., 2015). We obtained 5-point BET_{Ar} surface areas as tabulated in Table 1. The BET_{Ar} of CFA_UK had the highest SSA of 14 $m^2 g^{-1}$, which was a factor of 3 higher than the other CFA particles: CFA_Cy (5 $m^2 g^{-1}$), CFA_Mi (4 $m^2 g^{-1}$), CFA_Ja (4 $m^2 g^{-1}$), and CFA_Wh (3 $m^2 g^{-1}$). The high SSA of CFA_UK is indicative of the presence of crevices in form of pores or grooves and therefore could account for the ice nucleation enhancement exhibited by the pre-activated CFA_UK particles compared to the other CFA particle types in this study. Note that this does not necessarily mean that all particles with high SSA such as soot particles will show pre-activation and ice nucleation enhancement. For example, pre-activation was not observed for water-processed soot particles (Wagner et al., 2016a), however, other soot types have been suspected to show considerable ice activity via the PCF mechanism (Mahrt et al., 2018; Wagner et al., 2016b).

We also report the pore volume (PV) of these particles (Table 1). The PV was calculated with a DFT/Monte Carlo model assuming that the pore diameters are not greater than 100 nm. In our results, CFA_UK had the highest PV (0.05 $cm^3 g^{-1}$), about 4 to 5 times higher compared to the other CFA samples. Although other CFA samples reported lower PV than CFA_UK, there was no clear correlation with their ice nucleation enhancement. For example, CFA_Ja and CFA_Wh had the same PV (0.009 $cm^3 g^{-1}$) but CFA_Wh showed a higher ice enhancement behaviour than the former. Also, the PV of CFA_Cy (0.012 $cm^3 g^{-1}$) is almost the same as CFA_Mi yet CFA_Cy showed a clear ice enhancement behaviour as CFA_Wh, which has a lower PV. Specific surface areas correlate with the PV (Sigmund et al., 2017), however, it is difficult to ascertain the geometries of the pores or crevices contributing to the surface area. CFA particles are very unique particles in that some of them can be cenospheres (hollow particles with a tiny opening). They can also have plerospheres, i.e. a case whereby smaller particles fill the larger cenospheres (Alegbe et al., 2018; Goodarzi, 2006; Goodarzi and Sanei, 2009). The cenospheres and plerospheres could increase the pore volume of these particles, hence, leading to a higher uncertainty in estimating the pore size. Therefore, we considered it pointless to estimate the pore sizes based on the PV of the CFA samples except in the case of a well-defined pore model and morphology. We suggest that knowing the possible geometries of defects on the surface of INPs may help to predict their pre-activation behaviour.

3.3 Potential implication of CFA particles pre-activation in clouds

Ice nucleation by CFA particles pre-activated via the PCF mechanism could be important for different cloud types. When CFA particles are lofted into the atmosphere, these particles can act as INPs or CCN as well as sinks for other atmospheric species (Dlugi and Güsten, 1983; Havlíček et al., 1993; Herndon, 2016; Korfmacher et al., 1980; Muduli et al., 2014). Depending on the transport of CFA particles in the atmosphere, they can pass through different altitudes and temperature regimes which can naturally provide a temperature-cycling and freezing process for these particles to be pre-activated. There is a high potential that the pre-activated CFA particles can be re-circulated as INPs via rainout or sedimentation (Hong et al., 2004) into the lower atmosphere to contribute to ice formation in mixed-phase clouds as illustrated in Fig. 8. Some of the atmospheric processes that could aid the re-circulation of the pre-activated INPs are radiative cooling and deep convective

flows (Highwood and Hoskins, 1998; Salathé et al., 1997). By convective atmospheric dynamics, these particles could then be released to lower altitudes and trigger ice formation at warmer temperatures than intrinsically expected. In addition, some CFA particles that initiated cloud glaciation can also be released via cloud evaporation or the sublimation of the ice particles releasing the CFA ice residues back into the atmosphere. These pre-activated CFA INPs can then re-initiate cloud formation at warmer temperatures than intrinsically expected for the same CFA INPs. This process is not peculiar to CFA particles, but also relevant for other natural and anthropogenic INPs with unique properties such as illite NX, zeolite, and GSG soot that exhibit PCF mechanism and can have a wider atmospheric implication in cloud formation.

There is a need by the modelling community to study the impact that pre-activated INPs or INPs with ice-filled pores can have on cloud formation processes. Some observations show that more ice particles are observed at warmer temperatures than the amount expected by the available INPs (Hobbs and Rangno, 1985). Aside from the secondary ice multiplication processes (Hallett and Mossop, 1974; Phillips et al., 2018), it could be possible that pre-activated INPs also contribute to the higher concentration of ice crystals that are observed in some cases. Currently, this is not well understood and requires further research. There are other open questions in these areas such as understanding the timescale and frequency (often or episodic) that this phenomenon occurs in the cloud, the impact of this processing in mixed-phase and cirrus clouds formation, and studying the dominance of this occurrence at regional and global levels. The PCF mechanism could be potentially important for cirrus cloud system because CFA particles entrained into the upper troposphere at lower temperatures could already have their pores filled with ice. For instance, our experiment with CFA_UK particles at 228 K showed over 70 % ice activation (Fig. 3D).

4. Conclusions

Coal fly ash (CFA) aerosol particles inherently nucleate ice in the immersion freezing mode as shown from this investigation and in previous studies. However, an exposure of these particles to favourable atmospheric conditions such as cold temperatures (~ 228 K) at ice sub-saturated conditions can induce the formation of ice germs in the pores or crevices of the CFA particles by the pore condensation and freezing (PCF) mechanism. The ice-filled cavities in the CFA aerosol particles can then account for their improved ice nucleation efficiencies at higher temperatures, where intrinsically, CFA will only show considerable or no ice formation. This behaviour could be attributed to the degree of surface defects, porosity, and chemical compositions of such CFA particles, which differ from sample to sample. In this study, we have clearly shown that CFA_UK particles are capable of enhancing their ice formation potential up to about 264 K by a factor of 2 for the condensational growth and even higher when they form ice by the depositional growth mode of the pre-existing ice germs. We have described the seemingly observed immersion freezing after the temperature-cycling procedure as caused by the condensational growth of the ice germs, while the apparent deposition freezing is triggered by the depositional growth of the ice germs in the pores.

A more in-depth study in understanding the temperatures and relative humidity ranges in which the ice in the pores can be preserved is important in quantifying their overall ice-nucleating efficiencies, depending on their temperature and relative humidity histories during atmospheric transport. This will clearly define the viability of INPs to form ice via the PCF mechanism. We suggest that further studies should be focused on investigating the effect of different pore geometries on their ice-nucleating abilities via the PCF mechanism. This can have a wider application in the modelling of cloud formation processes, and would help in constraining the uncertainties associated in the Earth system interactions e.g. aerosol-cloud interactions. We also suggest that to overcome the bias associated with pore models in estimating pore sizes for natural aerosol particles, a parameter based on the pore volume and specific surface area should be adopted. There is still a lot to be investigated to understand the PCF phenomena. Here are some open questions in this theme: (1) How do the pore geometries

influence the PCF mechanism? This could be useful in predicting the behaviour of INPs in different tropospheric conditions. (2) At what temperature and relative humidity conditions will the pre-activated ice sublime/melt or become ineffective in triggering ice formation? (3) What timescale does a potential INP needs to be exposed to lower temperatures for pre-activation to occur? (4) What are the typical temperatures and relative humidity histories that aerosol particles experience during atmospheric transport? and (5) Aside from the atmospheric implications, how well do we understand this process for other applications, especially in cryopreservation, bioengineering, and agriculture.

Data availability: All data shown in this report will be available via KITopen or contact <nsikanabasi.umo@partner.kit.edu>.

Author contributions: NSU and RW designed and conducted the experiments with contributions from OM, RU, HS. NSU, RW, RU, TL, AK, DC, and OM analysed the data and discussed the ice nucleation results. PGW characterised the BET and pore volume of the samples and led the discussions of the results. AK and NSU took the SEM images and discussed the morphology of the particles. NSU prepared the manuscripts with contributions from all the co-authors (RW, RU, AK, HS, PGW, DC, TL, and OM). OM hosted and provided a complementary funding for the project.

Competing interests: The authors declare that they have no conflict of interest.

Acknowledgements: N. S. Umo acknowledges Alexander von Humboldt Foundation, Germany (1188375) for funding this project and generously thanks IMK-AAF, KIT for access to the AIDA Cloud/Aerosol Simulation Chamber and other instrumentation. We are thankful to the AIDA technical team at IMK-AAF, KIT for their assistance in operating the AIDA chamber, specifically, George Scheurig, Steffen Vogt, Tomasz Chudy, Rainer Buschbacher, and Olga Dombrowski. We thank Professor (Emeritus) Alan Williams of the University of Leeds for providing one of the CFA samples. Part of this work was funded by the Helmholtz Association of German Research Centres through its Atmosphere and Climate Programme.

Any opinions, findings, and conclusions or recommendations expressed in this material are those of the author(s) and do not necessarily reflect the views of the Alexander von Humboldt Foundation.

References

Adams, T. H.: Coal Ash Recycling Reaches Record 64 Percent Amid Shifting Production and Use Patterns. [online] Available from: www.acaa-usa.org (Accessed 4 January 2019), 2018.

Alegbe, J., Ayanda, O. S., Ndungu, P., Alexander, N., Fatoba, O. O., and Petrik, L. F.: Chemical, Mineralogical and Morphological Investigation of Coal Fly Ash Obtained from Mpumalanga Province, South Africa, Res. J. Environ. Sci., 12(3), 98–105, https://doi.org/10.3923/rjes.2018.98.105, 2018.

Benz, S., Megahed, K., Möhler, O., Saathoff, H., Wagner, R., and Schurath, U.: T-dependent rate measurements of homogeneous ice nucleation in cloud droplets using a large atmospheric simulation chamber, J. Photochem. Photobiol. A Chem., 176(1–3), 208–217, https://doi.org/10.1016/J.JPHOTOCHEM.2005.08.026, 2005.

Blissett, R. S. and Rowson, N. A.: A review of the multi-component utilisation of coal fly ash, Fuel, 97, 1–23, https://doi.org/10.1016/J.FUEL.2012.03.024, 2012.

Boucher, O., Randall, D., Artaxo, P., Bretherton, C., Feingold, G., Forster, P., Kerminen, V.-M., Kondo, Y., Liao, H., Lohmann, U., Rasch, P., Satheesh, S. K., Sherwood, S., Stevens, B., and Zhang, X. Y.: Clouds and Aerosols, Cambridge University Press, Cambridge, United Kingdom, 2013.

Brunauer, S., Emmett, P. H., and Teller, E.: Adsorption of Gases in Multimolecular Layers, J. Am. Chem. Soc., 60, 309–

319 https://doi.org/10.1021/ja01269a023, 1938.

Campbell, J. M. and Christenson, H. K.: Nucleation- and Emergence-Limited Growth of Ice from Pores, Phys. Rev. Lett., 120(16), 165701, https://doi.org/10.1103/PhysRevLett.120.165701, 2018.

Campbell, J. M., Meldrum, F. C., and Christenson, H. K.: Observing the formation of ice and organic crystals in active sites, Proc. Natl. Acad. Sci., 114(5), 810–815, https://doi.org/10.1073/pnas.1617717114, 2017.

Dlugi, R. and Güsten, H.: The catalytic and photocatalytic activity of coal fly ashes, Atmos. Environ., 17(9), 1765–1771, https://doi.org/10.1016/0004-6981(83)90183-X, 1983.

Fahey, D. W., Gao, R. S., Möhler, O., Saathoff, H., Schiller, C., Ebert, V., Krämer, M., Peter, T., Amarouche, N., Avallone, L. M., Bauer, R., Bozóki, Z., Christensen, L. E., Davis, S. M., Durry, G., Dyroff, C., Herman, R. L., Hunsmann, S., Khaykin, S. M., Mackrodt, P., Meyer, J., Smith, J. B., Spelten, N., Troy, R. F., Vömel, H., Wagner, S., and Wienhold, F. G.: The AquaVIT-1 intercomparison of atmospheric water vapor measurement techniques, Atmos. Meas. Tech., 7(9), 3177–3213, https://doi.org/10.5194/amt-7-3177-2014, 2014.

Fisher, G. L., Prentice, B. A., Silberman, D., Ondov, J. M., Biermann, A. H., Ragaini, R. C., and McFarland, A. R.: Physical and morphological studies of size-classified coal fly ash, Environ. Sci. Technol., 12(4), 447–451, https://doi.org/10.1021/es60140a008, 1978.

Fukuta, N.: Activation of Atmospheric Particles as Ice Nuclei in Cold and Dry Air., J. Atmos. Sci., 23(6), 741–750, https://doi.org/10.1175/1520-0469(1966)023<0741:AOAPAI>2.0.CO;2, 1966.

Garimella, S.: A vertically-integrated approach to climate science: from measurements and machine learning to models and policy, Ph.D Thesis, Massachusetts Institute of Technology, 2016.

Goodarzi, F.: Characteristics and composition of fly ash from Canadian coal-fired power plants, Fuel, 85(10–11), 1418–1427, https://doi.org/10.1016/j.fuel.2005.11.022, 2006.

Goodarzi, F. and Sanei, H.: Plerosphere and its role in reduction of emitted fine fly ash particles from pulverized coal-fired power plants, Fuel, 88(2), 382–386, https://doi.org/10.1016/j.fuel.2008.08.015, 2009.

Grawe, S., Augustin-Bauditz, S., Hartmann, S., Hellner, L., Pettersson, J. B. C., Prager, A., Stratmann, F., and Wex, H.: The immersion freezing behavior of ash particles from wood and brown coal burning, Atmos. Chem. Phys., 16(21), 13911–13928, https://doi.org/10.5194/acp-16-13911-2016, 2016.

Grawe, S., Augustin-Bauditz, S., Clemen, H. C., Ebert, M., Eriksen Hammer, S., Lubitz, J., Reicher, N., Rudich, Y., Schneider, J., Staacke, R., Stratmann, F., Welti, A., and Wex, H.: Coal fly ash: Linking immersion freezing behavior and physicochemical particle properties, Atmos. Chem. Phys., 18(19), 13903–13923, https://doi.org/10.5194/acp-18-13903-2018, 2018.

Gregg, S. J., Sing, K. S. W., and Salzberg, H. W.: Adsorption Surface Area and Porosity, J. Electrochem. Soc., 114(11), 279C, https://doi.org/10.1149/1.2426447, 1967.

Hallett, J. and Mossop, S. C.: Production of secondary ice particles during the riming process, Nature, 249(5452), 26–28, https://doi.org/10.1038/249026a0, 1974.

Havlíček, D., Přibil, R., and Školoud, O.: The chemical and mineralogical composition of the water-soluble fraction of power-plant ash and its effect on the process of crystallization of water, Atmos. Environ. Part A, Gen. Top., 27(5), 655–660, https://doi.org/10.1016/0960-1686(93)90183-Y, 1993.

He, Z., Liu, K. and Wang, J.: Bioinspired Materials for Controlling Ice Nucleation, Growth, and Recrystallization, Acc. Chem. Res., 51(5), 1082–1091, https://doi.org/10.1021/acs.accounts.7b00528, 2018.

Heidrich, C., Feuerborn, H.-J., and Weir, A.: Coal Combustion Products : a global perspective, in World of Coal Ash Conference, p. 17. [online] Available from: http://www.flyash.info/ (Accessed 4 January 2019), 2013.

Herndon, J. M.: Obtaining evidence of coal fly ash content in weather modification (geoengineering) through analyses of post-aerosol-spraying rainwater and solid substances, Indian J. Sci. Res. Technol., 4(1), 30–36 [online] Available from: www.indjsrt.com (Accessed 28 September 2018), 2016.

Heymsfield, A. J., Miloshevich, L. M., Schmitt, C., Bansemer, A., Twohy, C., Poellot, M. R., Fridlind, A., and Gerber, H.: Homogeneous Ice Nucleation in Subtropical and Tropical Convection and Its Influence on Cirrus Anvil Microphysics, J. Atmos. Sci., 62(1), 41–64, https://doi.org/10.1175/JAS-3360.1, 2005.

Highwood, E. J. and Hoskins, B. J.: The tropical tropopause, Q. J. R. Meteorol. Soc., 124(549), 1579–1604, https://doi.org/10.1002/qj.49712454911, 1998.

Hiranuma, N., Adachi, K., Bell, D., Belosi, F., Beydoun, H., Bhaduri, B., Bingemer, H., Budke, C., Clemen, H.-C., Conen, F., Cory, K., Curtius, J., DeMott, P., Eppers, O., Grawe, S., Hartmann, S., Hoffmann, N., Höhler, K., Jantsch, E., Kiselev, A., Koop, T., Kulkarni, G., Mayer, A., Murakami, M., Murray, B., Nicosia, A., Petters, M., Piazza, M., Polen, M., Reicher, N., Rudich, Y., Saito, A., Santachiara, G., Schiebel, T., Schill, G., Schneider, J., Segev, L., Stopelli, E., Sullivan, R., Suski, K., Szakáll, M., Tajiri, T., Taylor, H., Tobo, Y., Weber, D., Wex, H., Whale, T., Whiteside, C., Yamashita, K., Zelenyuk, A., and Möhler, O.: A comprehensive characterization of ice nucleation by three different types of cellulose particles immersed in water: lessons learned and future research directions, Atmos. Chem. Phys. Discuss., https://doi.org/10.5194/acp-2018-933, in review, 2018.

Hobbs, P. V. and Rangno, A. L.: Ice Particle Concentrations in Clouds, J. Atmos. Sci., 42(23), 2523–2549, https://doi.org/10.1175/1520-0469(1985)042<2523:IPCIC>2.0.CO;2, 1985.

Hong, S., Dudhia, J. and Chen, S.: A Revised Approach to Ice Microphysical Processes for the Bulk Parameterization of Clouds and Precipitation, Mon. Weather Rev., 132(1), 103–120, https://doi.org/10.1175/1520-0493(2004)132<0103:ARATIM>2.0.CO;2, 2004.

Hoose, C. and Möhler, O.: Heterogeneous ice nucleation on atmospheric aerosols: a review of results from laboratory experiments, Atmos. Chem. Phys., 12(20), 9817–9854, https://doi.org/10.5194/acp-12-9817-2012, 2012.

Isono, B. K. and Ikebe, Y.: On the ice-nucleating ability of rock-forming minerals and soil particles, J. Meteorol. Soc. Jpn., 38(5), 213–230, https://doi.org/10.2151/jmsj1923.38.5_213, 1960.

John Morris, G. and Acton, E.: Controlled ice nucleation in cryopreservation – A review, Cryobiology, 66(2), 85–92, https://doi.org/10.1016/J.CRYOBIOL.2012.11.007, 2013.

Joshi, R. and Lohita, R.: Fly ash in concrete: production, properties and uses. Gordon and Breach Science Publishers, Australia, 1997.

Kiani, H. and Sun, D.-W.: Water crystallization and its importance to freezing of foods: A review, Trends Food Sci. Technol., 22(8), 407–426, https://doi.org/10.1016/J.TIFS.2011.04.011, 2011.

Kiselev, A., Bachmann, F., Pedevilla, P., Cox, S. J., Michaelides, A., Gerthsen, D., and Leisner, T.: Active sites in heterogeneous ice nucleation-the example of K-rich feldspars., Science, 355(6323), 367–371, https://doi.org/10.1126/science.aai8034, 2017.

Knopf, D. A. and Koop, T.: Heterogeneous nucleation of ice on surrogates of mineral dust, J. Geophys. Res., 111(D12), D12201, https://doi.org/10.1029/2005JD006894, 2006.

Korfmacher, W. A., Wehry, E. L., Mamantov, G., and Natusch, D. F. S.: Resistance to photochemical decomposition of polycyclic aromatic hydrocarbons vapor-adsorbed on coal fly ash, Environ. Sci. Technol., 14(9), 1094–1099, https://doi.org/10.1021/es60169a019, 1980.

Landers, J., Gor, G. Y., and Neimark, A. V.: Density functional theory methods for characterization of porous materials, Colloids Surfaces A Physicochem. Eng. Asp., 437, 3–32, https://doi.org/10.1016/J.COLSURFA.2013.01.007, 2013.

Li, C., Tao, R., Luo, S., Gao, X., Zhang, K., and Li, Z.: Enhancing and Impeding Heterogeneous Ice Nucleation through Nanogrooves, J. Phys. Chem. C, 122(45), 25992–25998, https://doi.org/10.1021/acs.jpcc.8b07779, 2018.

Mahrt, F., Marcolli, C., David, R. O., Grönquist, P., Barthazy Meier, E. J., Lohmann, U., and Kanji, Z. A.: Ice nucleation abilities of soot particles determined with the Horizontal Ice Nucleation Chamber, Atmos. Chem. Phys., 18(18), 13363–13392, https://doi.org/10.5194/acp-18-13363-2018, 2018.

Manz, O. E.: Coal fly ash: A retrospective and future look, Fuel, 78(2), 133–136, https://doi.org/10.1016/S0016-2361(98)00148-3, 1999.

Marcolli, C.: Deposition nucleation viewed as homogeneous or immersion freezing in pores and cavities, Atmos. Chem. Phys., 14(4), 2071–2104, https://doi.org/10.5194/acp-14-2071-2014, 2014.

Marcolli, C.: Pre-activation of aerosol particles by ice preserved in pores, Atmos. Chem. Phys., 17(3), 1595–1622, https://doi.org/10.5194/acp-17-1595-2017, 2017.

Mason, B. J. and Maybank, J.: Ice-nucleating properties of some natural mineral dusts, Q. J. R. Meteorol. Soc., 84(361), 235–241, https://doi.org/10.1002/qj.49708436104, 1958.

Möhler, O., Stetzer, O., Schaefers, S., Linke, C., Schnaiter, M., Tiede, R., Saathoff, H., Krämer, M., Mangold, A., Budz, P., Zink, P., Schreiner, J., Mauersberger, K., Haag, W., Kärcher, B., and Schurath, U.: Experimental investigation of homogeneous freezing of sulphuric acid particles in the aerosol chamber AIDA, Atmos. Chem. Phys., 3(1), 211–223, https://doi.org/10.5194/acp-3-211-2003, 2003.

Möhler, O., Büttner, S., Linke, C., Schnaiter, M., Saathoff, H., Stetzer, O., Wagner, R., Krämer, M., Mangold, A., Ebert, V., and Schurath, U.: Effect of sulfuric acid coating on heterogeneous ice nucleation by soot aerosol particles, J. Geophys. Res., 110(D11), D11210, https://doi.org/10.1029/2004JD005169, 2005.

Muduli, S. D., Nayak, B. D., Dhal, N. K., and Mishra, B. K.: Atmospheric CO_2 Sequestration through Mineral Carbonation of Fly Ash, Greener J. Phys. Sci., 4(1), 1–6, doi:http://www.gjournals.org/GJPS/GJPS PDF/2014/January/102113913 Muduli et al.pdf, 2014.

Murray, B. J., O'Sullivan, D., Atkinson, J. D., and Webb, M. E.: Ice nucleation by particles immersed in supercooled cloud droplets, Chem. Soc. Rev., 41(19), 6519, https://doi.org/10.1039/c2cs35200a, 2012.

Murray, B. J.: Cracking the problem of ice nucleation., Science, 355(6323), 346–347, https://doi.org/10.1126/science.aam5320, 2017.

Phillips, V. T. J., Patade, S., Gutierrez, J., and Bansemer, A.: Secondary ice production by fragmentation of freezing drops: formulation and theory, J. Atmos. Sci., 75(9), JAS-D-17-0190.1, https://doi.org/10.1175/JAS-D-17-0190.1, 2018.

Prospero, J. M.: Long-range transport of mineral dust in the global atmosphere: impact of African dust on the environment of the southeastern United States., Proc. Natl. Acad. Sci. U. S. A., 96(7), 3396–403, https://doi.org/10.1073/PNAS.96.7.3396, 1999.

Pruppacher, H. R. and Klett, J. D.: Microphysics of clouds and precipitation, Springer, Netherlands, 2010.

Rouquerol, F., Rouquerol, J., and Sing, K. S. W.: Adsorption by powders and porous solids, Academic Press, Cambridge, USA, 2014.

Salathé, E. P., Hartmann, D. L., Jr., E. P. S., and Hartmann, D. L.: A Trajectory Analysis of Tropical Upper-Tropospheric Moisture and Convection, J. Clim., 10(10), 2533–2547, https://doi.org/10.1175/1520-0442(1997)010<2533:ATAOTU>2.0.CO;2, 1997.

Schmitt, T.: Homogeneous Freezing of Water Droplets and its Dependence on Droplet Size, Diploma Thesis, Karlsruhe Institute Of Technology (KIT), 2014.

Schnell, R. C., Van Valin, C. C., and Pueschel, R. F.: Atmospheric ice nuclei: No detectable effects from a coal-fired

powerplant plume, Geophys. Res. Lett., 3(11), 657–660, https://doi.org/10.1029/GL003i011p00657, 1976.

Seinfeld, J. H. and Pandis, S. N.: Atmospheric chemistry and physics : from air pollution to climate change. John Wiley, Chichester, United Kingdom, 2006.

Sigmund, G., Hüffer, T., Hofmann, T., and Kah, M.: Biochar total surface area and total pore volume determined by N_2 and CO_2 physisorption are strongly influenced by degassing temperature, Sci. Total Environ., 580, 770–775, https://doi.org/10.1016/j.scitotenv.2016.12.023, 2017.

Steinke, I., Möhler, O., Kiselev, A., Niemand, M., Saathoff, H., Schnaiter, M., Skrotzki, J., Hoose, C., and Leisner, T.: Ice nucleation properties of fine ash particles from the Eyjafjallajökull eruption in April 2010, Atmos. Chem. Phys., 11, 12945-12958, https://doi.org/10.5194/acp-11-12945-2011, 2011.

Steinke, I., Funk, R., Busse, J., Iturri, A., Kirchen, S., Leue, M., Möhler, O., Schwartz, T., Schnaiter, M., Sierau, B., Toprak, E., Ullrich, R., Ulrich, A., Hoose, C., and Leisner, T.: Ice nucleation activity of agricultural soil dust aerosols from Mongolia, Argentina, and Germany, J. Geophys. Res. Atmos., 121(22), 13,559-13,576, https://doi.org/10.1002/2016JD025160, 2016.

Storelvmo, T. and Tan, I.: MetZet Classic Papers The Wegener-Bergeron-Findeisen process-Its discovery and vital importance for weather and climate, Meteo. Zeit 24(4), 455-461, https://doi.org/10.1127/metz/2015/0626, 2015.

Suski, K. J., Bell, D. M., Hiranuma, N., Möhler, O., Imre, D., and Zelenyuk, A.: Activation of intact bacteria and bacterial fragments mixed with agar as cloud droplets and ice crystals in cloud chamber experiments, Atmos. Chem. Phys., 18, 17497-17513, https://doi.org/10.5194/acp-18-17497-2018, 2018

Thommes, M., Smarsly, B., Groenewolt, M., Ravikovitch, P. I., and Neimark, A. V.: Adsorption hysteresis of nitrogen and argon in pore networks and characterization of novel micro- and mesoporous silicas, Langmuir, 22(2), 756–764, https://doi.org/10.1021/la051686h, 2006.

Thommes, M., Kaneko, K., Neimark, A. V., Olivier, J. P., Rodriguez-Reinoso, F., Rouquerol, J., and Sing, K. S. W.: Physisorption of gases, with special reference to the evaluation of surface area and pore size distribution (IUPAC Technical Report), Pure Appl. Chem., 87(9–10), 1051–1069, https://doi.org/10.1515/pac-2014-1117, 2015.

Ullrich, R., Hoose, C., Möhler, O., Niemand, M., Wagner, R., Höhler, K., Hiranuma, N., Saathoff, H., Leisner, T., Ullrich, R., Hoose, C., Möhler, O., Niemand, M., Wagner, R., Höhler, K., Hiranuma, N., Saathoff, H., and Leisner, T.: A New Ice Nucleation Active Site Parameterization for Desert Dust and Soot, J. Atmos. Sci., 74(3), 699–717, https://doi.org/10.1175/JAS-D-16-0074.1, 2017.

Umo, N. S., Murray, B. J., Baeza-Romero, M. T., Jones, J. M., Lea-Langton, A. R., Malkin, T. L., O'Sullivan, D., Neve, L., Plane, J. M. C., and Williams, A.: Ice nucleation by combustion ash particles at conditions relevant to mixed-phase clouds, Atmos. Chem. Phys., 15(9), 5195–5210, https://doi.org/10.5194/acp-15-5195-2015, 2015.

Vali, G.: Quantitative Evaluation of Experimental Results an the Heterogeneous Freezing Nucleation of Supercooled Liquids, J. Atmos. Sci., 28(3), 402–409, https://doi.org/10.1175/1520-0469(1971)028<0402:qeoera>2.0.co;2, 1971.

Vali, G., DeMott, P. J., Möhler, O., and Whale, T. F.: Technical Note: A proposal for ice nucleation terminology, Atmos. Chem. Phys., 15(18), 10263–10270, https://doi.org/10.5194/acp-15-10263-2015, 2015.

Wagner, Möhler, O., Saathoff, H., Schnaiter, M., Skrotzki, J., Leisner, T., Wilson, T. W., Malkin, T. L., and Murray, B. J.: Ice cloud processing of ultra-viscous/glassy aerosol particles leads to enhanced ice nucleation ability, Atmos. Chem. Phys., 12(18), 8589–8610, doi:10.5194/acp-12-8589-2012, 2012.

Wagner, R., Linke, C., Naumann, K. H., Schnaiter, M., Vragel, M., Gangl, M., and Horvath, H.: A review of optical measurements at the aerosol and cloud chamber AIDA, J. Quant. Spectrosc. Radiat. Transf., 110(11), 930–949, https://doi.org/10.1016/j.jqsrt.2009.01.026, 2009.

Wagner, R., Kiselev, A., Möhler, O., Saathoff, H., and Steinke, I.: Pre-activation of ice-nucleating particles by the pore condensation and freezing mechanism, Atmos. Chem. Phys., 16(4), 2025–2042, https://doi.org/10.5194/acp-16-2025-2016, 2016.

Welti, A., Lüönd, F., Stetzer, O., and Lohmann, U.: Influence of particle size on the ice nucleating ability of mineral dusts, Atmos. Chem. Phys., 9, 6705-6715, https://doi.org/10.5194/acp-9-6705-2009, 2009

Whale, T. F., Holden, M. A., Kulak, A. N., Kim, Y.-Y., Meldrum, F. C., Christenson, H. K., and Murray, B. J.: The role of phase separation and related topography in the exceptional ice-nucleating ability of alkali feldspars, Phys. Chem. Chem. Phys., 19(46), 31186–31193, doi:10.1039/C7CP04898J, 2017.

Young, K. C.: Microphysical processes in clouds, Oxford University Press, Oxford, United kingdom, 1993.

Atmos. Chem. Phys. Discuss., https://doi.org/10.5194/acp-2019-7
Manuscript under review for journal Atmos. Chem. Phys.
Discussion started: 25 January 2019

Atmospheric Chemistry and Physics Discussions

Tables

Table 1: Sources, specific surface areas, pore volume, and the median diameter of coal fly ash aerosol particles used in this study. Argon gas was used for the BET measurements; hence, it is labelled as BET_{Ar}. The details of the samples and labels are given in section 2.1. The countries that the samples originated from are the United Kingdom (UK) and the United States of America (USA).

Sample labels	Country of origin	BET_{Ar} Specific surface area [m^2/g]	Specific Pore volume *(~up to 100 nm pore size)* [cm^3/g]	Median diameter of the CFA particles [µm]
CFA_UK	UK	14	0.053	0.47
CFA_Cy	USA	5	0.012	0.66
CFA_Mi	USA	4	0.013	0.42
CFA_Ja	USA	4	0.010	0.68
CFA_Wh	USA	3	0.009	0.66

Table 2: Information on the various ice nucleation experiments conducted during two distinct AIDA measurement campaigns named CAINIC01 and EXTRA18. Experiments (1 - 11) were conducted with unprocessed CFA particles while experiments (12 – 30) were performed with processed CFA particles (i.e., after the temperature-cycling process involving intermediate cooling to ~ 228 K, see section 2.5). The freezing mode mentioned here as based on the classification presented in Vali et al. (2015).

S/No.	Campaign/ Experiment name	CFA Samples	Start temperature (T_{start}) before the expansion (K)	Concentration of CFA particles in the AIDA chamber before the expansion (cm^{-3})	Dominant ice nucleation mode observed (based on classical definitions in Vali et al. 2015)
Experiments before the temperature-cycling process (Unprocessed particles)					
1	CAINIC01_10	CFA_UK	228	225	Deposition
2	CAINIC01_13	CFA_UK	261	189	Immersion
3	CAINIC01_14	CFA_UK	253	218	Immersion
4	CAINIC01_17	CFA_UK	243	183	Immersion
5	EXTRA18_03	CFA_UK	245	218	Immersion
6	EXTRA18_04	CFA_UK	241	209	Immersion/ Deposition
7	EXTRA18_22	CFA_UK	243	226	Immersion/ Deposition
8	EXTRA18_05	CFA_Cy	251	175	Immersion
9	EXTRA18_06	CFA_Ja	251	219	Immersion
10	EXTRA18_14	CFA_Wh	248	228	Immersion
11	EXTRA18_15	CFA_Mi	250	195	Immersion
Experiments after the temperature-cycling process (Processed particles)					
12	CAINIC01_18	CFA_UK	250	523	Deposition
13	CAINIC01_19	CFA_UK	254	453	Deposition
14	CAINIC01_20	CFA_UK	256	396	Deposition/ Immersion
15	CAINIC01_21	CFA_UK	259	299	Immersion
16	CAINIC01_22	CFA_UK	264	195	Immersion
17	EXTRA18_23	CFA_UK	251	642	Deposition
18	EXTRA18_24	CFA_UK	254	589	Deposition
19	EXTRA18_25	CFA_UK	259	515	Deposition/ Immersion
20	EXTRA18_26	CFA_UK	263	442	Immersion
21	EXTRA18_28	CFA_Cy	253	625	Immersion/ Deposition
22	EXTRA18_29	CFA_Cy	257	532	Immersion
23	EXTRA18_30	CFA_Ja	249	650	Immersion
24	EXTRA18_31	CFA_Ja	256	543	Immersion
25	EXTRA18_32	CFA_Ja	259	448	Immersion
26	EXTRA18_33	CFA_Wh	249	578	Deposition/ Immersion
27	EXTRA18_34	CFA_Wh	256	486	Immersion
28	EXTRA18_35	CFA_Wh	259	405	Immersion
29	EXTRA18_36	CFA_Mi	249	612	Immersion
30	EXTRA18_37	CFA_Mi	255	536	Immersion

Atmos. Chem. Phys. Discuss., https://doi.org/10.5194/acp-2019-7
Manuscript under review for journal Atmos. Chem. Phys.
Discussion started: 25 January 2019

Atmospheric Chemistry and Physics Discussions

Figures

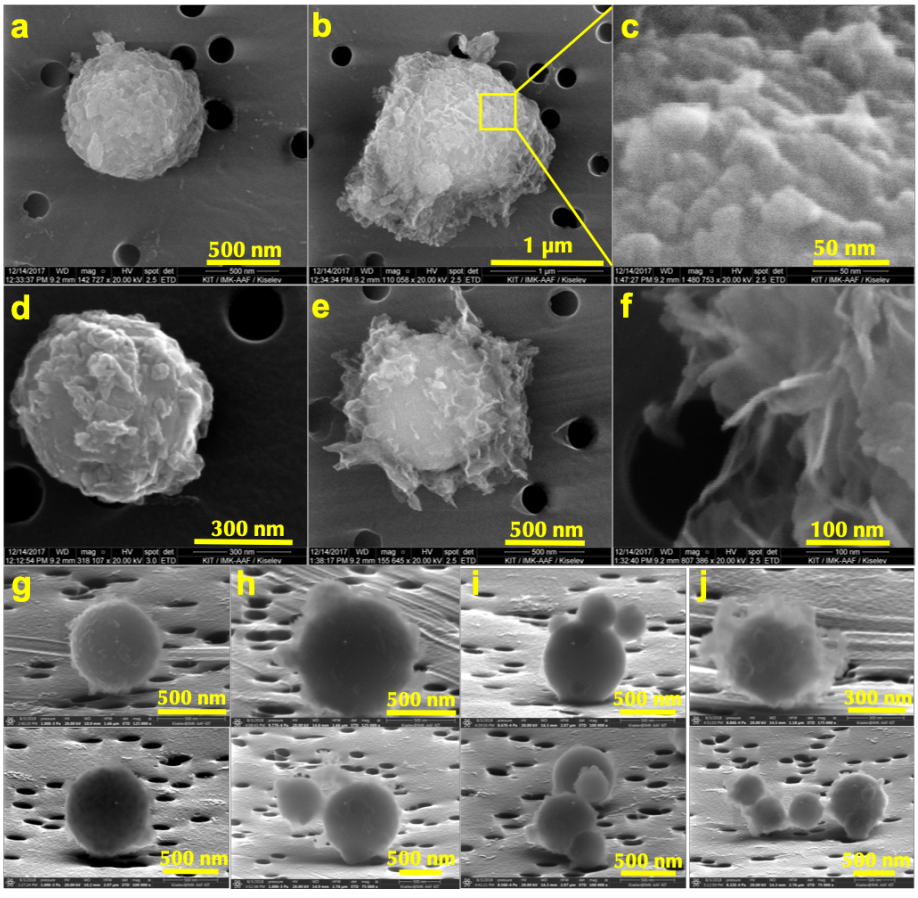

Figure 1: Scanning electron microscopy (SEM) images of CFA_UK particles (a - f), CFA_Cy (g), CFA_Mi (h), CFA_Ja (i), and CFA_Wh (j). All particles have a basic spherical shape, which is common to coal fly ash particles: (a) Spherical shape of CFA_UK with surface defects, (b) Meshy or spongy material on the particle surface which looks highly porous, (c) a high magnification image (~ 50 nm) of the pores or surface defects on the CFA_UK aerosol particles, (d) the core of CFA_UK shows a spherical shape like image (a) with scaly materials on the surface, (e) irrespective of the flake-like network materials on the surface of the CFA particles - the basic spherical core is still intact. (f) high magnification of the flaky, meshy stuff on the particles surface, (g) CFA_Cy particles also show some degree of deposits on the surface, (h) CFA_Mi with light meshy material compared to the CFA_UK, (i) CFA_Ja particles with non-smooth surface, and (j) CFA_Wh particles with a denser flaky network material on the surface than the other USA CFA samples. Images of the USA CFA particles taken by Garimella (2016) also showed scaly materials on the surface of the particles. However, CFA_UK particles had more defects and materials on the surface which were very irregularly-shaped.

Atmos. Chem. Phys. Discuss., https://doi.org/10.5194/acp-2019-7
Manuscript under review for journal Atmos. Chem. Phys.
Discussion started: 25 January 2019

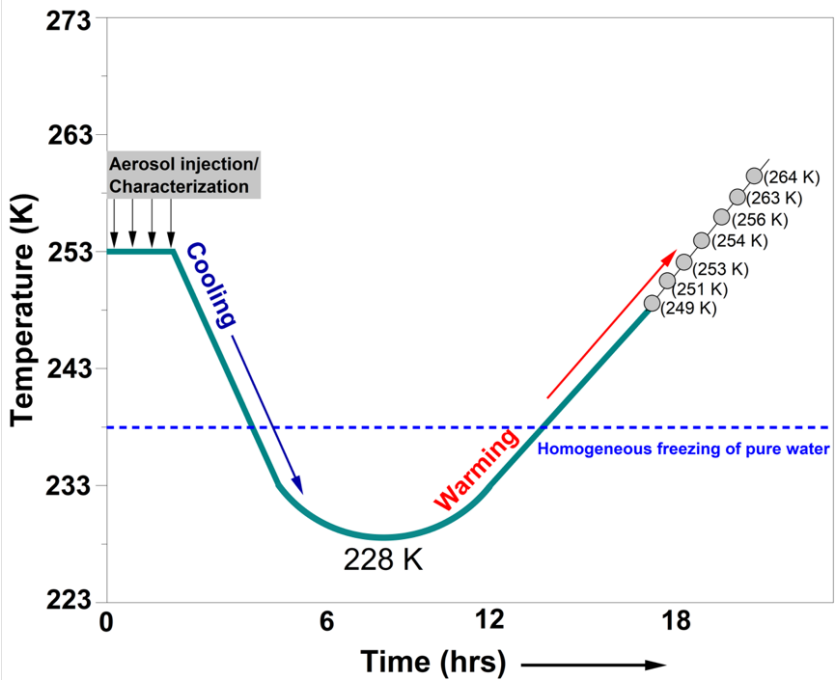

Figure 2: A schematic showing the temperature-cycling and freezing (TCF) process. The temperatures indicated by the grey circles are the start temperatures (T_{start}) for the ice nucleation experiments conducted after the warming. For a particular CFA sample, experiments were not conducted at all start temperatures indicated on this schematic. That depended on the degree of activity observed at the previous temperature. The x-axis denotes the overall timescale of the procedure. The homogeneous freezing line of pure water is an indication of the temperature where supercooled water droplets were observed to freeze in previous AIDA experiments (Benz et al., 2005; Schmitt, 2014).

Atmos. Chem. Phys. Discuss., https://doi.org/10.5194/acp-2019-7
Manuscript under review for journal Atmos. Chem. Phys.
Discussion started: 25 January 2019

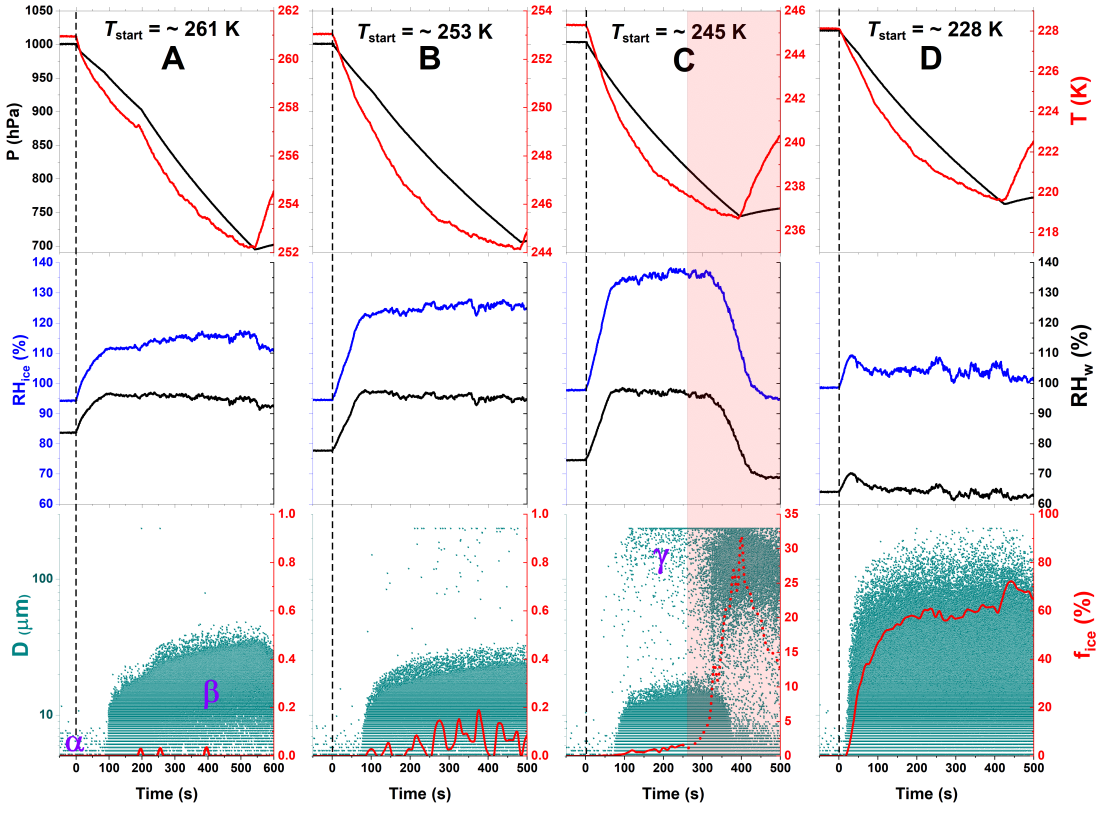

Figure 3: Ice nucleation experiment data for unprocessed CFA_UK particles at 261 K, 253 K, 245 K, and 228 K start temperatures (T_{start}). Each column (A, B, C, & D) has 3 plot panels – top, middle, and bottom. The top panels show the pressure (hPa, black) and the mean gas temperature (K, red) profiles of the AIDA aerosol and cloud simulation chamber throughout the duration of the experiment. The middle panels indicate the changes in the relative humidity with respect to ice (RH_{ice}, blue) and water (RH_w, black), both in %. The bottom panels illustrate the data for the optical size measurements from the OPCs (green dots). Greek letters point to the various types of particles detected, alpha, CFA seed aerosol particles, beta, cloud droplets, and gamma, ice crystals (see text for details). The bottom panels also include the ice-activated fraction (%) of the aerosol particle population (f_{ice}, red line). In column C (bottom panel, shaded region), there is a sudden increase in the number concentration of ice particles due to the onset of homogeneous freezing. The ice-activated fraction due to the homogeneous freezing of water droplets is denoted by the dashed red line to separate it from the heterogeneous immersion freezing mode.

Atmos. Chem. Phys. Discuss., https://doi.org/10.5194/acp-2019-7
Manuscript under review for journal Atmos. Chem. Phys.
Discussion started: 25 January 2019

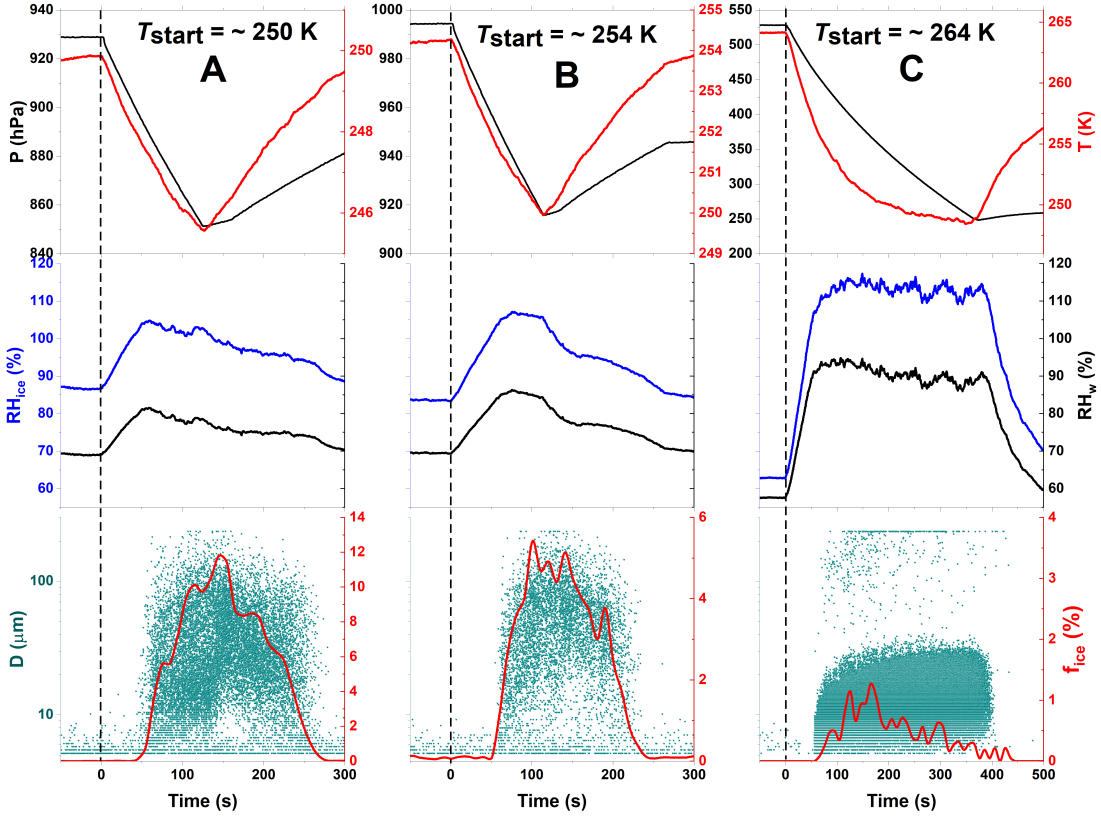

Figure 4: Freezing experiment data for processed CFA_UK particles at 250 K, 254 K, and 264 K start temperatures (T_{start}). Processing involved the intermediate cooling of the particles to 228 K (see Figure 2). The individual panels contain the same data types as in Figure 3.

Atmos. Chem. Phys. Discuss., https://doi.org/10.5194/acp-2019-7
Manuscript under review for journal Atmos. Chem. Phys.
Discussion started: 25 January 2019

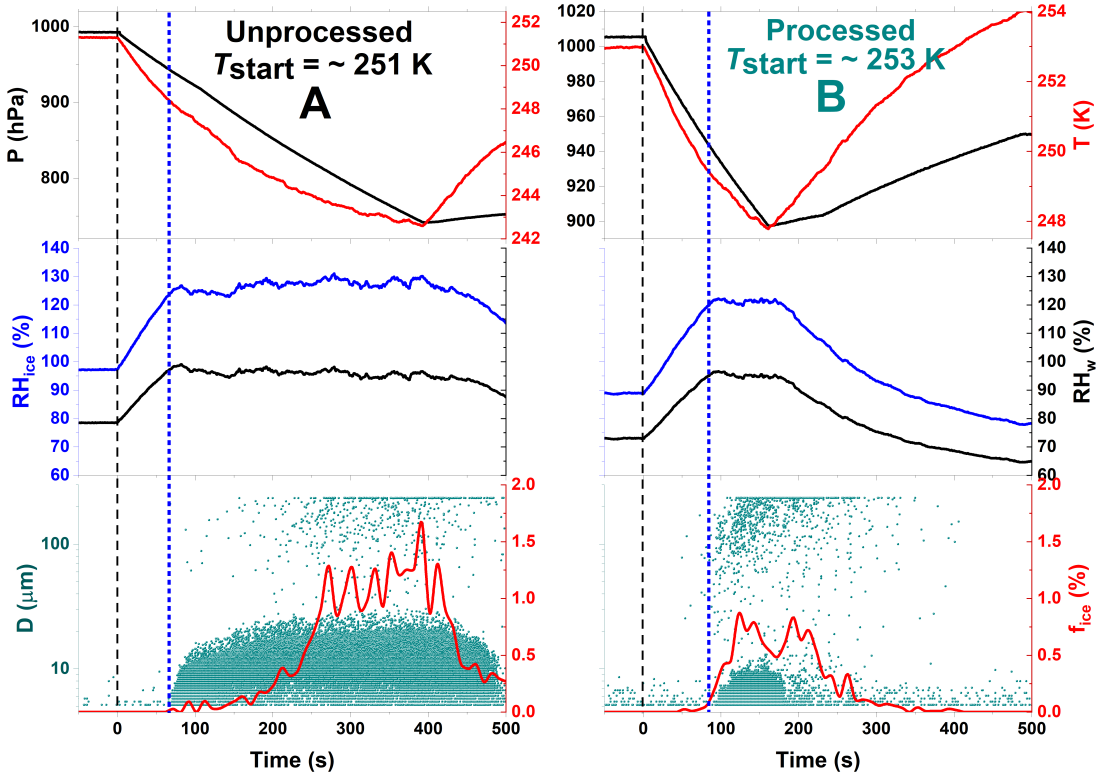

Figure 5: Freezing experiment data for unprocessed and processed CFA_Cy particles at 251 K and 253 K start temperatures (T_{start}). The individual panels contain the same data types as in Figure 3.

Atmos. Chem. Phys. Discuss., https://doi.org/10.5194/acp-2019-7
Manuscript under review for journal Atmos. Chem. Phys.
Discussion started: 25 January 2019

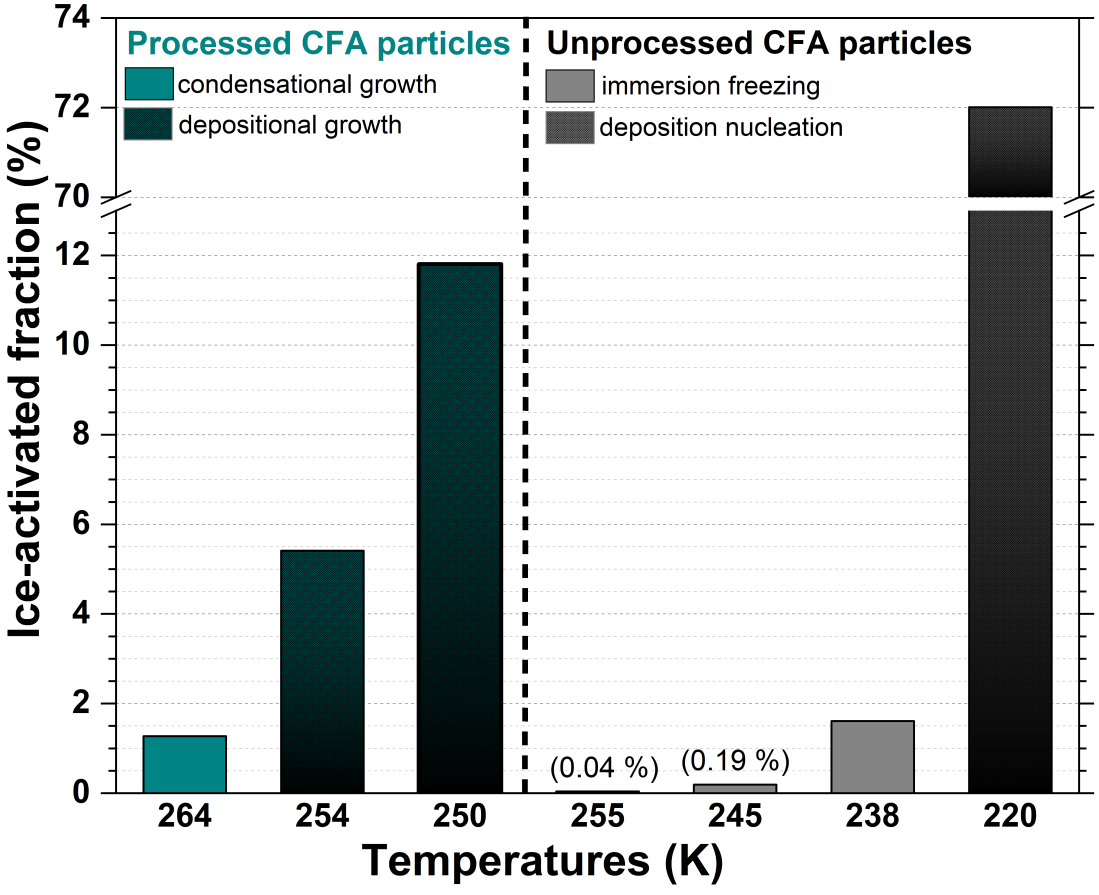

Figure 6: Summary of the ice-activated fraction (%) of unprocessed and processed CFA_UK particles as a function of temperature. The grey bars on the right-hand side of the plot indicate experiments before the TCF procedure and the dark cyan bars show experiments after the TCF process.

Atmos. Chem. Phys. Discuss., https://doi.org/10.5194/acp-2019-7
Manuscript under review for journal Atmos. Chem. Phys.
Discussion started: 25 January 2019

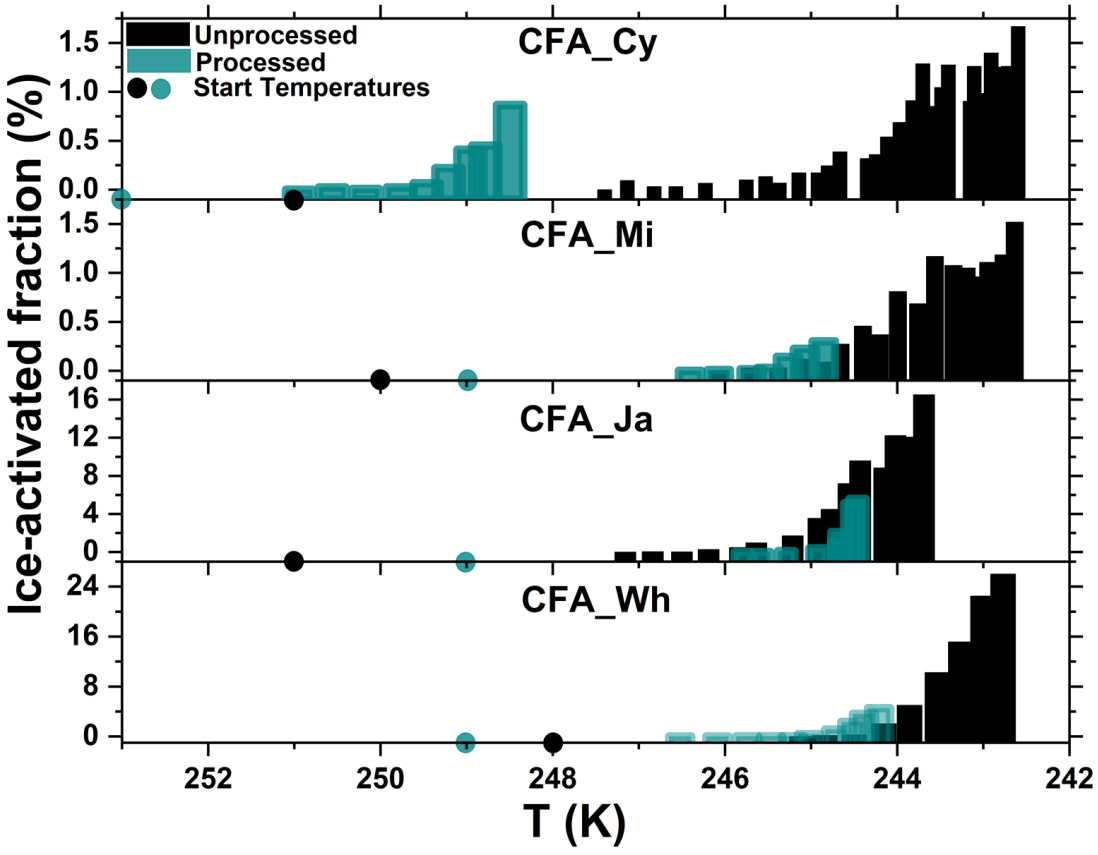

Figure 7: Summary of the ice-activated fraction (%) of unprocessed and processed CFA_Cy, CFA_Mi, CFA_Ja, and CFA_Wh particles as a function of temperature. The black bars show experiments before the temperature-cycling and freezing (TCF) procedure and the transparent dark cyan bars represent experiments after the TCF process.

Atmos. Chem. Phys. Discuss., https://doi.org/10.5194/acp-2019-7
Manuscript under review for journal Atmos. Chem. Phys.
Discussion started: 25 January 2019

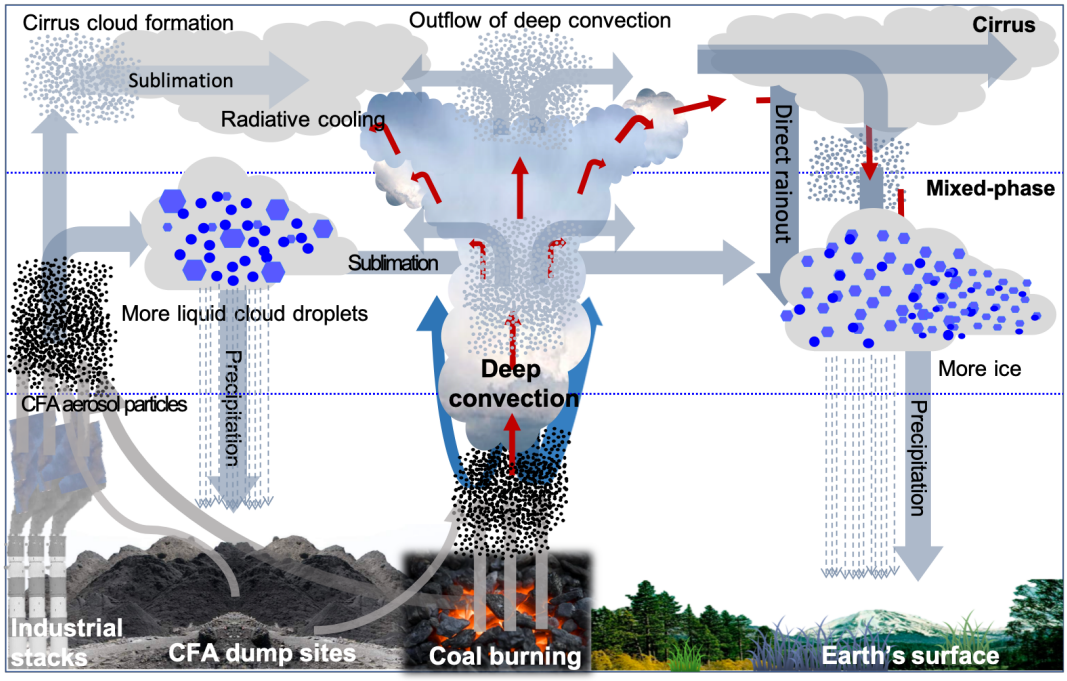

Figure 8: A schematic showing possible pathways and interactions of CFA particles in the atmosphere. From the emission of the particles to the atmosphere where they can directly trigger heterogeneous ice formation in both cirrus and mixed-phase clouds (left-hand-side). The processing of these particles through lower temperatures can promote ice formation by pore condensation and freezing mechanism (middle) and generally influence the hydrological cycle.